EPAM: Eversive Pneumatic Artificial Muscle

T. Abrar*, *Student Member, IEEE*, F. Putzu*, *Student Member, IEEE*, J. Konstantinova, *Member, IEEE* and K. Althoefer, *Member, IEEE*

***Abstract*— Pneumatic Artificial Muscles, which are lightweight actuators with inherently compliant behavior, are broadly recognized as safe actuators for devices that assist or interact with humans. This paper presents the design and implementation of a soft pneumatic muscle based on the eversion principle - Eversive Pneumatic Artificial Muscle (EPAM). The proposed pneumatic muscle exerts a pulling force when elongating based on the eversion (growing) principle. It is capable of extending its length by a minimum of 100% when fully inflated. In contrast to other soft pneumatic actuators, such as the McKibben muscle, which contract when pressurized, our EPAM extends when pressure is increased. Additionally, important advantages of employing the eversion principle are the capability to achieve high pulling forces and an efficient force to pressure ratio. In a pivoting joint/link mechanism configuration the proposed muscle provides motion comparable to human arm flexion and extension. In this work, we present the design of the proposed EPAM, study its behavior, and evaluate its displacement capability and generated forces in an agonistic and antagonistic joint/link arrangement. The developed EPAM prototype with a diameter of 25 mm and a length of 250 mm shows promising results, capable of exerting 10 N force when pressurized up to 62 KPa.**

I. Introduction

The development of soft pneumatic actuators attracts the attention of researchers worldwide [1]. Such types of actuators benefit from their simple design and prove to be low-cost. In contrast to electric motors, they are soft, lightweight and have a compliant actuation behavior. Therefore, they are highly suitable for applications that require safe physical interaction with the environment and, especially, with humans in close vicinity. Examples include wearable devices for healthcare, rehabilitation and physical assistance [2]–[5]. Soft pneumatic actuators are often used as Pneumatic Artificial Muscles (PAMs) employing the concept of converting pneumatic actuation into displacement. With the growing interest in creating solutions for safe human-robot interaction, the development of such artificial muscles is establishing itself as an important research topic [6], [7]. Most PAMs exhibit a linear displacement when actuated [8], [9]. Research into PAMs aims to improve their performance in terms of maximum force, force to pressure ratio, stroke length, air consumption, efficiency and durability [10]. In addition, as a pneumatically driven system, such air muscles need to be airtight to ensure maximum performance. Therefore, design and fabrication methods need to be tailored to ensure that the resulting air muscle structure is free from leaks at any desired pressure level.

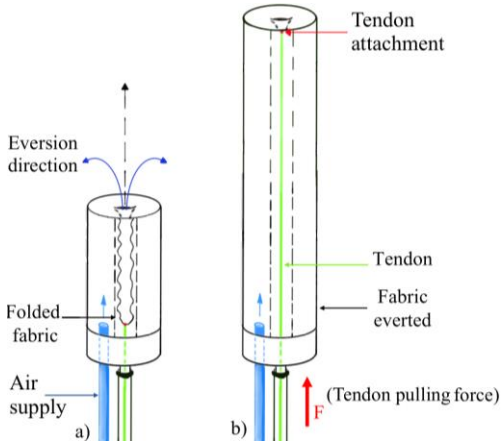

Figure 1. a) EPAM in relaxed state: the air supply pressurizes the folded muscle in the relaxed state causing the eversion motion; b) EPAM in extended state: the fabric everts together with the tendon that is applying a pulling force along the eversion direction.

Different artificial pneumatic muscles show a shortening or elongating behavior when the internal pressure is increased [11]. McKibben muscles are probably the most known and applied pneumatic muscles [11]. In several applications, they were successfully integrated with robotic arms to provide motion [10], [12], [13]. A common approach is to attach both ends of a McKibben muscle to two robot links connected via pivoting joint. Pressurizing such an integrated McKibben muscle leads to a muscle contraction that creates a rotary movement of the first link around the joint towards the second link [10], [14]. Pneumatic McKibben muscles use a stretchable cylindrical rubber chamber combined with a non-stretchable fiber mesh [15], [16]. These muscles can contract to approximately 20-25% of their length when pressurized [17]. The overall force that a McKibben muscle can achieve is limited by the strength of the used fiber mesh. In addition, the efficiency of the McKibben muscle is influenced by the counteracting forces of the inner elastic chamber.

Another example of artificial muscles, Series Pneumatic Artificial Muscles (SPAMs) are made from multiple polyethylene tubes, segmented by O-rings in order to create different chambers [18]. The working principle of the actuator is as follows: the tube is inflated, the segments elongate. It is possible to achieve soft bending structures by combining of multiple inflatable chambers. However, the integration and control of these muscles in a robotic system is challenging due to the use of multiple tubes and segments. Alternatively, Inverse

*Equally contributing authors.

T. Abrar, F. Putzu, J. Konstantinova and K. Althoefer are with the Centre for Advanced Robotics Lab @ Queen Mary, Faculty of Science and Engineering, Queen Mary University of London, London, E1 4NS, United Kingdom. (e-mail: {t.abrar; f.putzu; j.konstantinova; k.althoefer}@qmul.ac.uk).

Manuscript 38 submitted to 2019 2nd IEEE International Conference on Soft Robotics (RoboSoft). Received November 9, 2018.

Pneumatic Artificial Muscles (IPAMs) were developed in [9]. Such muscles use an elastic latex tube that is reinforced by a helical fiber structure. The latex is stretchable and allows the tube to extend and store energy when pressurized. The outer fiber wrapping restricts the muscle expansion in the radial direction. It is noted that the use of the elastic material for the tubes yields a nonlinear stress-strain curve; thus, complicating control. Another muscle prototype, Antagonistic Pneumatic Artificial Muscle (APAM) makes use of internal and external chambers to achieve an antagonistic behavior. While most actuators can be paired with an actuator of the same type to produce an antagonistic behavior, APAM is considered to be an actuator type that combines this behavior within a single actuator structure. However, they require both an air and a vacuum pump to achieve the antagonistic behavior [7].

All the above-mentioned muscles employ stretchable materials such as plastic or silicone that can lead to non-linearity and decrease durability. Another approach in the construction of artificial muscles is the use of fabric materials that can also apply high forces onto objects. Recently a trend to create articulated devices from fabric is observable [19]–[21]. The advantages of fabric-based actuated devices in rehabilitation were reported in recent works [3]–[5], [22]–[26]. In addition, fabric-based robots have shown their strengths for different tasks that includes grasping and manipulation [27]. In most of these robotic applications, the fabric is used as the constraining material. It is observed, that when fully pressurized a further increase in pressure leads to an increase in stiffness of the structure. Recent research [19], demonstrates the strength and payload capabilities of such fabric-based robots, namely a human finger size actuator exerting 7 N force at its tip. Therefore, fabric shows the high potential for fabrication of artificial pneumatic muscles.

In this paper we propose the fabric-based Eversive Pneumatic Artificial Muscle (EPAM) that elongates when pressure is applied to its internal chamber. When pressure is applied the muscle is increasing its length (growing) due to the eversion of the inwards folded fabric. The proposed EPAM has the following benefits:

- The fabric structure provides high compliance and makes it suitable for safe human-robot interaction.
- It operates at a safe low-pressure range (up to 83 KPa).
- The muscle can elongate multiple times beyond its folded unpressurized state outperforming standard pneumatic muscles.
- The force to pressure ratio is superior compared to other actuators, such as McKibben muscle.
- The stiffness of the EPAM is a function of applied pressure and attached load [28]; therefore, allowing stiffness controllability.
- The muscle provides a considerable strength to device weight ratio.
- In a joint/link mechanism configuration the muscle can reach an angle similar to a human arm flexion.

In the experimental study, we investigate and show the payload of the new actuator, as well as demonstrate its capabilities to exert force within a joint-link mechanism. Due to the above-mentioned features, the EPAM is suitable for the construction of robotic devices for rehabilitation, assistive technologies and collaborative robots. The next section discusses the design and construction of the proposed artificial pneumatic muscle. Further quantitative evaluation of the muscle is discussed in Section III. Section IV discusses the presented work and draws out conclusions.

II. Design

The proposed EPAM consists of an airtight fabric-reinforced bladder which folds inside-out at the tip when pressure is applied, as it is shown in Figure 1. In the relaxed state (Figure 1 a), when pressurized the fabric inside the sleeve is continuously pushed towards the tip and unfolds outwards (Figure 1 b). Therefore, during the process of actuation, the folded fabric that is inside is everted out to the outer surface.

To create the movement of an arm or link a pulling force should be generated. In our design, this function is implemented with an internal tendon, which is the key feature of the proposed EPAM [29]. The tendon is attached by sewing it to the tip of the artificial muscle from the inner side. Therefore, when pressurized it moves together with the tip as described above. This transforms the expanding properties of the muscle into a pulling force F, as shown in Figure 1.

A. Construction

Polyester ripstop (non-stretchable) fabric is used in the fabrication of our EPAM; it is lightweight (10 g per muscle) and allows the created structure to fold, bend and compliantly adapt to the environment [30]. Moreover, the used ripstop fabric is robust to tearing. The EPAM is fabricated from one strip of a fabric sheet (size 300 mm × 100 mm). The sheet is sewn to form a cylindrical shape. As a result, EPAM prototype is 250 mm in length and 25 mm in diameter after sewing. Afterwards, one of the two open ends is closed forming the tip of the muscle. To achieve the eversion effect, the tip is folded inside and the tendon is attached [29]. The other end is kept open for the air input.

Figure 2. Design of air stopper and anchor to ensure airtightness.

A layer of natural rubber is applied to the inside of the fabric cylinder, along the seams to ensure airtightness. In order to have a complete airtight structure avoiding also air leakage from the base of the EPAM (where the tendon passes through), an air stopper has been inserted. The air stopper (Figure 2) has an air supply inlet and a hole for the tendon to pass through, and it is located at the base of the EPAM. To ensure the smooth motion of the tendon, the tendon hole (0.2 mm) is slightly larger than the diameter of the tendon (0.14

mm). Therefore, some air leakage is still observed. To avoid this leakage, a 4mm radius fabric cover encapsulates the tendon from the tip of the air stopper to the anchor, as shown in Figure 2. The anchor is attached to the external link mechanism. The tendon cover is made from the same ripstop fabric and also sealed with natural rubber; when the muscle extends it folds in a harmonic way. The air stopper was designed and 3D printed, to fit our EPAM prototype. As a final step, the completed everting structure with the air stopper is encapsulated in the fabric cover with the length corresponding to the maximum extension of the EPAM.

B. Actuation of EPAM

In the human body, biceps and triceps work in antagonistic configuration. This means that when the biceps is contracted the triceps relaxes causing the flexion of the arm (Figure 2(a)). In contrary, when the triceps is contracted the biceps relaxes, and the arm becomes extended (Figure 2(c)). The biceps is located on the front part of the upper arm, while the triceps is located on the back part of the upper arm.

Investigating flexion, one EPAM is employed to achieve that comparable motion in a link-joint mechanism. Figure 2 shows how the EPAM is attached to a pivoting joint/link mechanism. When the EPAM is pressurized the muscle elongates and causes the arm flexion (Figure 2(b)). On the other hand, when the EPAM is depressurized the artificial muscle folds back and the attached link moves into a straight configuration because of gravity (Figure 2(d)). Relaxation of the natural muscle causes the forearm to be lowered while the EPAM is reducing in length when achieving the same type of lowering the forearm. However, in order to implement the controllability of extension, mimicking the functionality of triceps, a second EPAM can be added. Thus, an antagonistic behavior can be achieved.

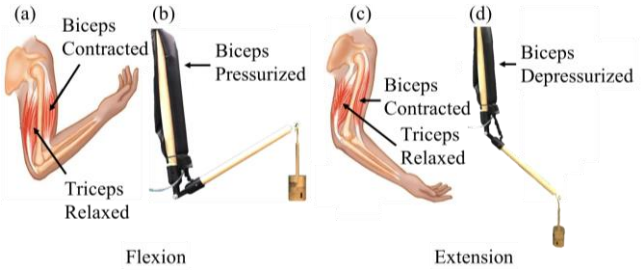

Figure 3. EPAM working in agonistic configuration: (a) the EPAM is depressurized and the arm is extended, (b) human arm with biceps relaxed and triceps contracted to create extension, (c) the EPAM pressurized (extended) causing the arm flexion, (d) human arm with biceps contracted and triceps relaxed to flex the arm.

The pneumatic actuation system of EPAMs consists of an air compressor with a maximum pressure range up to 350 KPa. However, it was found that the maximum pressure needed to achieve full inflation, as well as maximum stiffness was below 83 KPa. In addition, a pressure regulator (SMC ITV2050-212BL4) is required per each EPAM in order to achieve controllability. The pressure regulators are controlled by a microcontroller.

III. Performance Evaluation

In order to test the performance of the proposed EPAM, we have conducted an evaluation study exploring the following three configurations of artificial muscles: (1) a single muscle acting as a linear actuator (Figure 4(a)); (2) an agonistic configuration with a single muscle acting as a biceps (Figure 4(b)); and an antagonistic configuration with two muscles representing the equivalent of biceps and triceps of an arm (Figure 4(c)).

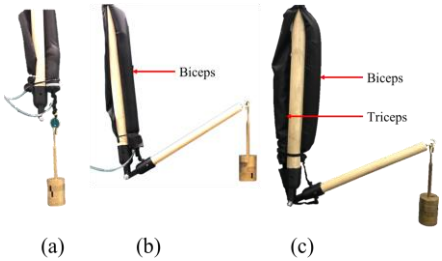

Figure 4. Experimental setup: (a) linear setup (b) as biceps (c) antagonistic configuration.

A joint/link mechanism was constructed to test our EPAM in a robot arm setting with a pivoting joint between the upper arm and the forearm. The individual components of the mechanism have the following dimensions: the upper arm is 30 mm in diameter and 350 mm long, and the forearm is 25 mm in diameter and 300 mm long. The joint can achieve a maximum rotation of 135°. The two arm elements are made from light wood with the weight of 50 g (upper arm) and 40 g (forearm), respectively. The performance of EPAM was evaluated based on the ability to lift payload, working pressure range as well as possible linear and angular displacement. In addition, a comparative study for agonistic configuration was conducted using a single McKibben muscle.

A. EPAM test as standalone actuator

In order to evaluate the performance of the single muscle, a standalone EPAM was tested without joint/link mechanism. As shown in Figure 4(a), weights were attached via the tendon to the tip of the EPAM. By pneumatically actuating the EPAM, a pulling force along the eversion direction was exerted, and the weight was lifted up. Therefore, the linear displacement can be evaluated. The applied force was increased in steps of 1 N from 0 N to 10 N, while the pneumatic pressure was increased from 0 KPa to 83 KPa, in steps of 7 KPa. The resultant maximum displacement is directly linked to the dimensions of the muscle and in this case is equal to 250 mm. This value equals to the maximum length of the EPAM.

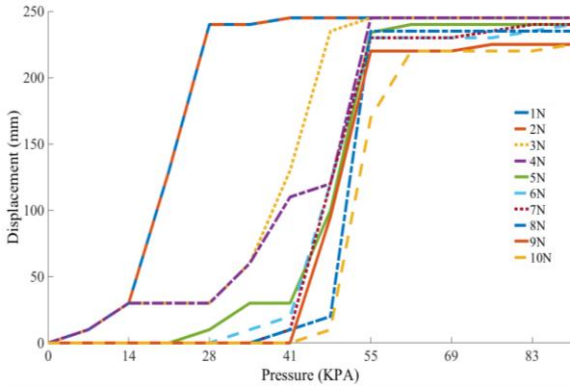

Figure 5. Performance of the standalone EPAM for different loads (1 to 10 N) in case of increasing internal pressure up to 83 KPa.

In order to evaluate the performance of the artificial muscle for lifting weights linearly up and down, experiments with increasing and decreasing pressures were performed. The results of experiments for lifting the weights are shown in Figure 5. Once the maximum distance was achieved, further pressure increase resulted in an increase of the stiffness of the EPAM. When the applied force reaches up to 9 N, there is no further displacement after the pressure of 55 KPa. For the case of the maximum load of 10 N, the maximum displacement is achieved at 62 KPa. In addition, the increase in pressure beyond the maximum displacement results in increase of the stiffness of the EPAM. Therefore, such configuration allows to lift the load, and also ensures robustness of the system capable of holding the load when required.

A similar, but flipped pattern is measured when the pressure is decreased with a step of 7 KPa starting from 83 KPa to 0 KPa (Figure 6). While extending the elbow joint it is observable that the muscle is able to hold the maximum load of 10 N with a minimum pressure of 41 KPa. Moreover, small loads up to 3 N can be held with a minimum pressure of just 10 KPa.

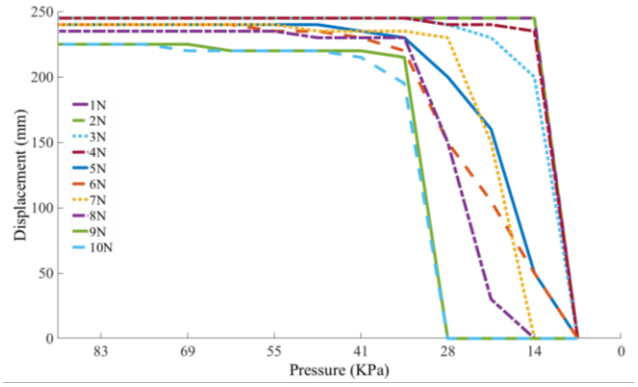

Figure 6. Performance of the standalone EPAM for different loads (1 to 10 N) in case of decreasing internal pressure from 83 KPa.

B. Testing of EPAM in agonistic configuration

As a proof of concept of a practical application in agonistic configuration, the EPAM was attached to a joint/link mechanism like a biceps (Figure 4(b)). The pressure applied inside the muscle defines the range of angular displacement of the load attached at the tip of the forearm. When the pressure is increased, the arm flexes, and when the pressure is decreased the arm extends (Figure 7).

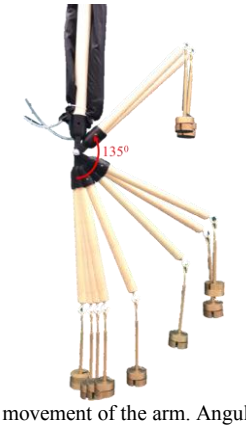

Figure 7. The agonistic movement of the arm. Angular displacement for the load of 3 N.

As it is shown in Figure 7, the effect of an incrementing pressure shows that the arm is able to reach and to keep different positions at different pressures. In this configuration, the tendon of the EPAM is attached at a distance of 45 mm on the forearm from the elbow. The connection location of the tendon influences the muscle payload capability, as it is described below. Due to the design constraints of the joint/link mechanism, the maximum possible angular displacement of 135° is achieved. This value compares well to the motion of the arm of a healthy human that can flex up to 145° [31]. To achieve the angular displacement the pressure is increased from 0 to 50 KPa with an increment of 7 KPa. However, it is observed that the relationship between the applied pressure increment and the angular displacement is not linear. Figure 8 shows the experimental results of the angular displacement with respect to the applied pressure in an agonist configuration. It was also noticed that in this configuration, the muscle started moving the arm and overcome the opposing forces when the input was 14 KPa for 3 N load. This pressure value is higher due to the angular displacement.

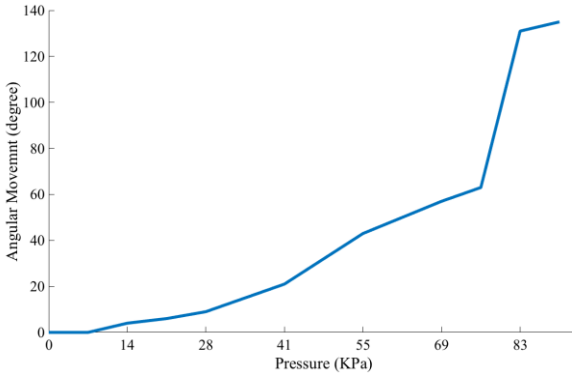

Figure 8. Angular displacement with respect to the applied pressure in agonistic configuration with a load of 3 N.

To describe the forces required for angular displacement, Figure 9 shows the diagram of the forces occurring in the system. The EPAM in agonistic configuration can be represented as an analogous lever system. During system equilibrium, in steady state, the total torque of the system is always zero [32]. The weight at the distal end of forearm creates clockwise torque τ_1 and the counterclockwise torque τ_2 created by EPAM. When these opposing torques become equal they cancel each other and make the arm stationary. Therefore, the force exerted by the artificial muscle F_A can be calculated as follows:

$$F_A = (F_P B + F_{fa} CG) / A, \qquad (1)$$

where A is the distance between the attachment of the tendon on the forearm and the elbow; B is the length of the forearm; and CG is the center of the gravity of the forearm. F_{fa} is force occurring due to the weight of the forearm, and F_P is the force from the weight P attached at the tip of the forearm. Assuming the applied load is 3 N, it can be calculated that the force on bicep equals to 21.7 N. The relationship of the exerted force and the load supported is the ratio of F_A and the total weight of the forearm and the load. It was found that our

EPAM exerts a force that is 6.4 times higher than the total weight when lifting 3 N.

In order to understand the maximum force exerted by the EPAM in the agonistic configuration, the weight and the resultant force F_P was increased until the maximum angular displacement of 135° was maintained. It was found that 5 N was the maximum possible load. Therefore, using the equation above, the maximum required force exerted by the muscle to achieve an equilibrium is 34.4 N. In addition, the exerted force to total weight ratio remains the same with a value of 6.4, which was also for 3 N payload. This demonstrates a linear behavior of the system over this range.

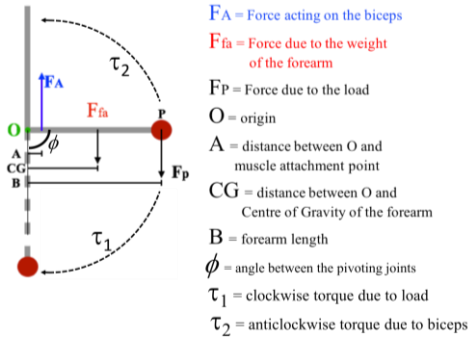

Figure 9. Forces acting on the arm in agonist configuration.

1) Comparison with McKibben muscle

To compare the performance of our EPAM with the state-of-the-art artificial muscle an experiment with a McKibben muscle was performed. The muscle used was attached to the upper arm of the joint/link mechanism in an agonistic configuration. The McKibben muscle was constructed with the same dimension as the EPAM: 25 mm in diameter and 250 mm in length. When inflated at the same pressure range used to actuate our EPAM, the McKibben muscle contracted only up to 20%, comparing reasonably well with the literature [17], with an elbow joint angle of maximum 90°. This angle was achieved when the load is up to 1 N. For increased load the elbow joint angle significantly reduces; for instance, it equals 45° for a load of 3 N. The observed differences in angular displacement and payload can be explained with the low contraction value of McKibben muscle. While our EPAM is extending up to 100% in the proposed system.

C. Antagonistic Configuration

As described in Section II.B, the human arm works in antagonistic fashion with biceps and triceps. To mimic this antagonistic actuation principle, a second EPAM is added to the agonistic setup in joint/link mechanism (Figure 4(c)). For this configuration, the focus is on extending the arm (moving downwards) against the force exerted by the biceps. To do this, the triceps input must be greater than the input of the biceps. To verify this concept a load of 3 N is applied at the distal end of the forearm. Further on, the biceps is actuated at a constant pressure (P_x) for all the tested values up to 83 KPa with a step of 7 KPa. As a result, the forearm link flexes at an angle as discussed in Section III.B. Further on, the triceps is actuated incrementally at the same pressure ranges up to 83 KPa. It is confirmed that the triceps is unable to extend the arm until it reaches an internal pressure (P_y) greater than the biceps. The measured relationship between the two antagonistic muscles is linear, as it is shown in Figure 10. This linearity with regards to the R^2 value of 0.9956 is as follows:

$$P_y = 3.7P_x - 11.8 \quad (2)$$

In this configuration the maximum force exerted by the EPAM is also equal to 5 N as it is for the agonistic configuration. However, compared to the agonistic configuration it shows a better controlled angular displacement for arm extensions, as the triceps is acting as a support for the joint. This is due to the pulling force generated by the triceps during arm extension.

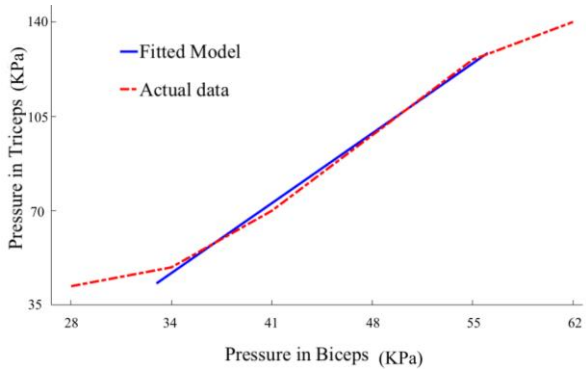

Figure 10. Triceps and biceps pressure relationship in an antagonistic configuration using two EPAMs.

TABLE I. CHARACTERISTIC FEATURES OF THE EPAM

Feature	Quantity		Feature	Quantity
Actuation	Pneumatic		Pressure range	0 - 83 KPa
Folded length	125 mm		Maximum elongation	250 mm
Exerted force (biceps)	34.4 N		Mass of the muscle	10 g
Maximum joint angle (biceps)	135°		Safe interraction	Yes
Scalable	Yes			

IV. DISCUSSION AND CONCLUSION

In this paper the new concept of an artificial muscle based on eversion is proposed. We have experimentally evaluated the payload and pulling force capability of the EPAM in several practical configurations, including standalone muscle, agonistic setup with biceps only, as well as using two muscles to create antagonistic biceps and triceps behavior. Advantages of the presented EPAM include its low weight (in our case: of 10g) and natural compliance due to fabric-based, inflatable structure. Moreover, the proposed EPAM can be easily scaled for the desired application purposes. We have observed the linear relationship of pressure and exerted force, with a maximum payload capability of 5 N for agonistic and antagonistic configuration for our prototype. Moreover, our EPAM in a standalone configuration is able to lift up to 10 N. The EPAM in a joint/link configuration can lift 6.4 times more weight than what the whole EPAM structure weighs.

Moreover, the proposed muscle benefits from low cost and easy manufacturing. It is noted that the manufacturing is complicated by the requirement of complete airtightness. This issue is solved by applying a latex layer on the seams of

the everting structure. Like every pneumatic device, continuous air supply is required, as the loss of power can lead to the collapse of the whole structure.

Compared to the performance of the human muscle and the common McKibben pneumatic muscle which increase their stiffness when contracted, the EPAM becomes stiffer whilst extending. We have shown that with our EPAM a link/joint arrangement can achieve angular displacement that compare well to the motion performance of a human arm with upper and lower arm pivoting around the elbowWith the improvement in the mechanical design of the elbow joint in our system, higher values of angular displacement are expected to be achieved. The characteristic features of our EPAM are presented in Table I.

ACKNOWLEDGMENT

This work was supported in part by the EPSRC National Centre for Nuclear Robotics project (EP/R02572X/1), the Innovate UK WormBot project (104059) and the Innovate UK project iGrasp (103676).

REFERENCES

[1] F. Daerden and D. Lefeber, "Pneumatic Artificial Muscles: actuators for robotics and automation," p. 11.

[2] R. V. Martinez, A. C. Glavan, C. Keplinger, A. I. Oyetibo, and G. M. Whitesides, "Soft Actuators and Robots that Are Resistant to Mechanical Damage," *Adv. Funct. Mater.*, vol. 24, no. 20, pp. 3003–3010, May 2014.

[3] H. K. Yap, J. H. Lim, F. Nasrallah, and C.-H. Yeow, "Design and Preliminary Feasibility Study of a Soft Robotic Glove for Hand Function Assistance in Stroke Survivors," *Front. Neurosci.*, vol. 11, pp. 1–9, 2017.

[4] H. K. Yap, J. H. Lim, J. C. H. Goh, and C.-H. Yeow, "Design of a Soft Robotic Glove for Hand Rehabilitation of Stroke Patients with Clenched Fist Deformity Using Inflatable Plastic Actuators," *J. Med. Devices*, vol. 10, no. 4, p. 044504, 2016.

[5] P. Polygerinos, K. C. Galloway, E. Savage, M. Herman, K. O. Donnell, and C. J. Walsh, "Soft robotic glove for hand rehabilitation and task specific training," *2015 IEEE Int. Conf. Robot. Autom. ICRA*, vol. 2015-June, no. June, pp. 2913–2919, 2015.

[6] M. Memarian, R. Gorbet, and D. Kulic, "Modelling and experimental analysis of a novel design for soft pneumatic artificial muscles," 2015, pp. 1718–1724.

[7] N. Usevitch, A. M. Okamura, and E. W. Hawkes, "APAM: Antagonistic Pneumatic Artificial Muscle," p. 8.

[8] J. Wirekoh and Y.-L. Park, "Design of flat pneumatic artificial muscles," *Smart Mater. Struct.*, vol. 26, no. 3, p. 035009, 2017.

[9] E. W. Hawkes, D. L. Christensen, and A. M. Okamura, "Design and implementation of a 300% strain soft artificial muscle," 2016, pp. 4022–4029.

[10] G. Andrikopoulos, G. Nikolakopoulos, and S. Manesis, "Design and development of an exoskeletal wrist prototype via pneumatic artificial muscles," *Meccanica*, vol. 50, no. 11, pp. 2709–2730, Nov. 2015.

[11] P. Lopez and B. Tondu, "The McKibben muscle and its use in actuating robot- arms showing similarities with human arm behaviour," *Ind. Robot Int. J.*, vol. 24, no. 6, pp. 432–439, Dec. 1997.

[12] F. Sorge, "Dynamical behaviour of pneumatic artificial muscles," *Meccanica*, vol. 50, no. 5, pp. 1371–1386, May 2015.

[13] R. Morita, H. Nabae, G. Endo, and K. Suzumori, "A proposal of a new rotational-compliant joint with oil-hydraulic McKibben artificial muscles," *Adv. Robot.*, vol. 32, no. 9, pp. 511–523, May 2018.

[14] D. Shin, X. Yeh, and O. Khatib, "Variable Radius Pulley Design Methodology for Pneumatic Artificial Muscle-Based Antagonistic Actuation Systems," p. 6.

[15] O. Erin, N. Pol, L. Valle, and Y.-L. Park, "Design of a bio-inspired pneumatic artificial muscle with self-contained sensing," 2016, pp. 2115–2119.

[16] Y. Liu, X. Zang, X. Liu, and L. Wang, "Design of a biped robot actuated by pneumatic artificial muscles," *Biomed. Mater. Eng.*, vol. 26, no. s1, pp. S757–S766, Aug. 2015.

[17] A. Al-Ibadi, S. Nefti-Meziani, and S. Davis, "Efficient Structure-Based Models for the McKibben Contraction Pneumatic Muscle Actuator: The Full Description of the Behaviour of the Contraction PMA," *Actuators*, vol. 6, no. 4, p. 32, Oct. 2017.

[18] J. D. Greer, T. K. Morimoto, A. M. Okamura, and E. W. Hawkes, "Series pneumatic artificial muscles (sPAMs) and application to a soft continuum robot," 2017, pp. 5503–5510.

[19] T. Abrar, F. Putzu, and K. Althoefer, "Soft Wearable Glove for Tele-Rehabilitation Therapy of Clenched Hand/Fingers Patients," presented at the Computer/Robot Assisted Surgery (CRAS), London, 2018, vol. 8th, p. 2.

[20] F. Putzu, T. Abrar, and K. Althoefer, "Development of a Soft Inflatable Structure with Variable Stiffness for Hand Rehabilitation," presented at the Computer/Robot Assisted Surgery (CRAS), London, vol. 8th, p. 2.

[21] A. Stilli, L. Grattarola, H. A. Wurdemann, and K. Althoefer, "Variable Stiffness Links (VSL): Toward Inherently Safe Robotic Manipulators," p. 6.

[22] P. Polygerinos, S. Lyne, Wang Zheng, L. F. Nicolini, B. Mosadegh, G. M. Whitesides, & C. J. Walsh, "Towards a soft pneumatic glove for hand rehabilitation," 2013, pp. 1512–1517.

[23] P. Polygerinos, Z. Wang, K. C. Galloway, R. J. Wood, and C. J. Walsh, "Soft robotic glove for combined assistance and at-home rehabilitation," *Robot. Auton. Syst.*, vol. 73, pp. 135–143, Nov. 2015.

[24] T. Kline, D. Kamper, and B. Schmit, "Control System for Pneumatically Controlled Glove to Assist in Grasp Activities," 2005, pp. 78–81.

[25] A. Hadi, K. Alipour, S. Kazeminasab, and M. Elahinia, "ASR glove: A wearable glove for hand assistance and rehabilitation using shape memory alloys," *J. Intell. Mater. Syst. Struct.*, pp. 1–11, 2017.

[26] H. K. Yap, N. Kamaldin, J. H. Lim, F. A. Nasrallah, J. C. H. Goh, and C. H. Yeow, "A Magnetic Resonance Compatible Soft Wearable Robotic Glove for Hand Rehabilitation and Brain Imaging," *IEEE Trans. Neural Syst. Rehabil. Eng.*, vol. 25, no. 6, pp. 782–793, 2017.

[27] J. M. Bern, G. Kumagai, and S. Coros, "Fabrication, modeling, and control of plush robots," 2017, pp. 3739–3746.

[28] M. E. Pontecorvo, F. S. Gandhi, and R. J. Niemiec, "Design studies on cellular structures with pneumatic artificial muscle inclusions for modulus variation," *J. Intell. Mater. Syst. Struct.*, vol. 27, no. 6, pp. 820–834, Apr. 2016.

[29] F. Putzu, T. Abrar, and K. Althoefer, "Plant-Inspired Soft Pneumatic Eversion Robot," in *2018 7th IEEE International Conference on Biomedical Robotics and Biomechatronics (Biorob)*, Enschede, Netherlands, 2018, pp. 1327–1332.

[30] A. Stilli, H. A. Wurdemann, and K. Althoefer, "Shrinkable, stiffness-controllable soft manipulator based on a bio-inspired antagonistic actuation principle," 2014, pp. 2476–2481.

[31] J. M. Soucie, C. Wang, A. Forsyth, S. Funk, M. Denny, K. E. Roach, D. Boone, The Hemophilia TREATMENT CENTER NETWORK, "Range of motion measurements: reference values and a database for comparison studies: NORMAL JOINT RANGE OF MOTION," *Haemophilia*, vol. 17, no. 3, pp. 500–507, May 2011.

[32] T. Bretl and S. Lall, "Testing Static Equilibrium for Legged Robots," *IEEE Trans. Robot.*, vol. 24, no. 4, pp. 794–807, Aug. 2008.